Published in final edited form as:
J Clin Cell Immunol. 2013 June 30; 4: . doi:10.4172/2155-9899.1000150.

Profile of Circulatory Metabolites in a Relapsing-remitting Animal Model of Multiple Sclerosis using Global Metabolomics

AK Mangalam[1,2,*], **LM Poisson**[3,4], **E Nemutlu**[5], **I Datta**[3,4], **A Denic**[2], **P Dzeja**[6], **M Rodriguez**[1,2], **R Rattan**[7], and **S Giri**[8,*]

[1]Department of Immunology, Mayo Clinic College of Medicine, Rochester, MN 55905, USA

[2]Department ofNeurology, Mayo Clinic College of Medicine, Rochester, MN 55905, USA

[3]Center for Bioinformatics, Henry Ford Health System, Detroit, MI 48202, USA

[4]Department of Public Health Sciences, Henry Ford Health System, Detroit, MI 48202, USA

[5]Department of Analytical Chemistry, Faculty of Pharmacy, University of Hacettepe, Ankara, Turkey

[6]Division of Cardiovascular Diseases, Molecular Pharmacology and Experimental Therapeutics, Mayo Clinic College of Medicine, Rochester, MN 55905, USA

[7]Division of Gynecology Oncology, Department of Women's Health Services, Henry FordHealth System, Detroit, MI 48202, USA

[8]Department of Neurology, Henry Ford Health System, Detroit MI48202, USA

Abstract

Multiple sclerosis (MS) is a chronic inflammatory and demyelinating disease of the CNS. Although, MS is well characterized in terms of the role played by immune cells, cytokines and CNS pathology, nothing is known about the metabolic alterations that occur during the disease process in circulation. Recently, metabolic aberrations have been defined in various disease processes either as contributing to the disease, as potential biomarkers, or as therapeutic targets. Thus in an attempt to define the metabolic alterations that may be associated with MS disease progression, we profiled the plasma metabolites at the chronic phase of disease utilizing relapsing remitting-experimental autoimmune encephalomyelitis (RR-EAE) model in SJL mice. At the chronic phase of the disease (day 45), untargeted global metabolomic profiling of plasma collected from EAE diseased SJL and healthy mice was performed, using a combination of high-throughput liquid-and-gas chromatography with mass spectrometry. A total of 282 metabolites were identified, with significant changes observed in 44 metabolites (32 up-regulated and 12 down-regulated), that mapped to lipid, amino acid, nucleotide and xenobiotic metabolism and distinguished EAE from healthy group ($p<0.05$, false discovery rate (FDR)<0.23). Mapping the differential metabolite signature to their respective biochemical pathways using the Kyoto Encyclopedia of Genes and Genomics (KEGG) database, we found six major pathways that were significantly altered (containing concerted alterations) or impacted (containing alteration in key junctions). These included bile acid biosynthesis, taurine metabolism, tryptophan and histidine metabolism, linoleic acid and D-arginine metabolism pathways. Overall, this study identified a 44

[*]**Corresponding authors:** Shailendra Giri, PhD, Department of Neurology, Research Division, Education & Research Building, Room 4051, Henry Ford Health System, 2799 West Grand Boulevard, Detroit, MI 48202, USA, Tel: (313) 916-7725; SGiri1@hfhs.org Ashutosh Mangalam, PhD, Department of Immunology and Neurology, Mayo Clinic College of Medicine, Rochester, MN 55905, USA; mangalam.ashutosh@mayo.edu.

Disclosures The authors have no financial conflict of interest.

metabolite signature drawn from various metabolic pathways which correlated well with severity of the EAE disease, suggesting that these metabolic changes could be exploited as (1) biomarkers for EAE/MS progression and (2) to design new treatment paradigms where metabolic interventions could be combined with present and experimental therapeutics to achieve better treatment of MS.

Keywords

Metabolomics; Plasma; Multiple sclerosis; Experimental autoimmune encephalitis; Biomarker; Metabolite signature; Metabolic pathways

Introduction

Multiple sclerosis (MS) is a chronic inflammatory and demyelinating disease of the central nervous system (CNS). The hypothesis, that MS is an autoimmune disease comes mainly from studies of an animal model for demyelination called experimental autoimmune encephalomyelitis (EAE) [1-3]. EAE can be induced in various inbred animal strains by inoculation of whole myelin or defined myelin proteins/peptides such as myelin basic protein (MBP), myelin oligodendrocyte glycoprotein (MOG), and proteolipod protein(PLP) in complete Freund's adjuvant (CFA) [1-3]. The two most widely used EAE models are the MOG_{35-55} induced chronic progressive EAE (C-EAE) in B6 mice and the $PLP_{139-151}$ induced relapsing remitting (RR-EAE) EAE in SJL mice.

Elegant studies in murine/rodent EAE models have documented that encephalitogenic T cells are $CD4^+$, T helper (Th1)-type cells secreting TNF-α/β and IFNγ [4-6]. However recent studies have indicated that a new T cell phenotype Th17 secreting IL-17, IL-17F, IL-21, IL-22 and IL-23 might also play an important role in the immuno-pathogenesis of EAE [7]. Thus current hypothesis of EAE indicates that both Th1 and Th17 cytokines play an important role in the immunopathogenesis of EAE. These encephalitogenic $CD4^+$ T cells traffic to CNS by crossing the leaky BBB (blood brain barrier) and initiate an inflammatory cascade, which ultimately leads to demyelination and possible axonal loss. To be efficacious as a therapeutic agent for EAE/MS, a drug should modulate directly or indirectly: i) Th1/Th17 pathway; ii) trafficking of inflammatory cells to CNS; and (iii) integrity of BBB. At the molecular level, a number of metabolites are generated inside and outside of the cells, which can directly or indirectly regulate immune response, and modulate inflammation and demyelination in CNS. Recent studies support this argument, as number of metabolites such as indoleamine 2,3-dioxygenase (IDO) [8], tryptophan, glucose and pyruvate have been shown to directly regulate CD4 T cells, macrophages and DC response [9-11].

Metabolomics focuses on global exploration of endogenous small molecule metabolites as the end products of cellular processes in the biological system, including cell, tissue, organ or organism [12,13]. Therefore, metabolic profiling can provide a window to the instantaneous as well as long term physiological or pathological changes as a supplement to the transcriptomic and proteomic profiling for the systematic and functional study of living organisms [14,15]. It has been used successfully in identifying novel clinical biomarkers and therapeutic targets, especially in cancer [16,17]. Recent reports have implicated the importance of metabolomics in the possible identification of biomarkers in neurological disorders including Alzheimer's disease [18,19], Parkinson's disease [20], and EAE using CSF and urine [21-23].

Here, we describe the first comprehensive analysis of plasma metabolites, using the $PLP_{139-151}$ induced RR-EAE model of MS, which mimics human RR-MS closely. This

study can be used as a surrogate for future studies to identify metabolites in the plasma of MS patients. We identified a 44 metabolite signature corresponding to various metabolite classes including lipids, amino acids, xenobiotics and carbohydrates that distinguishes the chronic phase of EAE disease from the non-disease state. Development of a non-invasive technique to measure disease severity quantitatively will greatly benefit the clinical and the scientific community and speed-up the drug development for MS patients.

Methods

Animals

Female SJL/J mice were purchased from Jackson Laboratories and housed in the pathogen-free animal facility of Mayo Clinic, Rochester, MN, according to the animal protocols approved by the Animal Care and Use Committee of Mayo Clinic.

Peptide and reagents

Murine myelin proteolipid protein ($PLP_{139-151}$; (HSLGKWLGHPDKF)) was synthesized at Mayo peptide core facility. Complete Freund's adjuvant (CFA) and mycobacterium tuberculosis (MT) lyophilized powder was purchased from DIFCO Laboratories (Michigan, USA).

EAE induction and recall response

SJL mice (10-12 wk old) were immunized on day 0 by subcutaneous (SC) injections in the flank region with total 200 μl of emulsion containing PLP139-151 peptide (100 μg/mouse), along with killed *Mycobacterium tuberculosis* H37Ra (400 μg). One set of mice were injected with CFA without $PLP_{139-151}$ peptide named as healthy. Clinical disease was monitored daily in a blinded fashion by measuring paralysis according to the conventional grading system: 0, no disease; 1, complete loss of tail tonicity; 2, partial hind limb paralysis (uneven gate of hind limb); 3, complete hind limb paralysis; 4, complete hind and forelimb paralysis; 5, moribund or dead. On day 45 (chronic phase of disease), cells (2×10^6/ml) isolated from lymph nodes of myelin $PLP_{139-151}$-immunized mice were cultured in the presence or absence of $PLP_{139-151}$ (20 μg/ml). Cell proliferation and the production of various cytokines (IFNγ and IL17) were examined as described before [24]. On the same day, blood was drawn from both groups to isolate plasma for metabolomics analysis.

Histology of the brain

Following perfusion with Trump's fixative, we made two coronal cuts in the intact brain at the time of removal from the skull (one section through the optic chiasm and a second section through the infundibulum). As a guide, we used the *Atlas of the Mouse Brain and Spinal Cord* corresponding to sections 220 and 350, page 664. These yielded three blocks that were embedded in paraffin to allow for systematic analysis of the pathology of the cortex, corpus callosum, hippocampus, brain stem, striatum, and cerebellum. The resulting slides were stained with hematoxylin and eosin (H&E) and assigned pathological scores to the different areas ofthe brain without knowledge of experimental group. We used a four-point scale to grade each area of the brain: 0, no pathology; 1, no tissue destruction but only minimal inflammation; 2, early tissue destruction (loss of architecture) and moderate inflammation; 3, definite tissue destruction (demyelination, parenchymal damage, cell death, neurophagia, neuronal vacuolation); and 4, necrosis (complete loss of all tissue elements with associated cellular debris). We assessed and graded meningeal inflammation as follows: 0, no inflammation; 1, one cell layer of inflammation; 2, two cell layers of inflammation; 3, three cell layers of inflammation; 4, four or more cell layers of

inflammation. The area with maximal tissue damage was used for assessment of each brain region.

Spinal cord pathology

We anesthetized mice with sodium pentobarbital and perfused them intracardially with Trump's fixative (phosphate-buffered 4% formaldehyde/1% glutaraldehyde, pH 7.4). We cut the removed spinal cords into 1 mm blocks with every third block postfixed and stained with osmium tetroxide and embedded in glycol methacrylate plastic (Polysciences, Warrington, PA). Ten to twelve spinal cord sections were stained with cresyl violet/ erichrome stain to visualize the myelin sheaths and inflammatory infiltrates. Each quadrant from every cross-section from each mouse was graded for the presence or absence of gray matter disease, meningeal inflammation, and demyelination. The score was expressed as the percentage of spinal cord quadrants examined with the pathological abnormality. A maximum score of 100 indicated a particular pathological abnormality in every quadrant of all spinal cord sections of a given mouse. All grading was performed on coded sections without knowledge of the experimental group.

Axon counts

Four sections of the mid-thoracic area were embedded in araldite plastic and stained with p-phenyldiamine. An Olympus Provis AX70 microscope that was fitted with a DP70 digital camera and a 60× oil-immersion objective was used to capture six sample areas of normal-appearing white matter containing a relative absence of demyelination from each cross section, according to the sampling scheme as previously reported [25]. Approximately 400,000 μm^2 of white matter was sampled from each mouse. Absolute myelinated axon numbers were calculated as previously reported [26]. Data were represented as the absolute number of all axons sampled per mid-thoracic spinal cord section. Data were analyzed without knowledge of experimental groups. All numbers were averaged per group.

Metabolomic Analysis

Metabolite analysis—Metabolomic profiling analysis was performed by Metabolon Inc. (Durham, NC) as previously described [17,27-29].

Sample accessioning—Each sample received was accessioned into the Metabolon LIMS system and was assigned by the LIMS a unique identifier that was associated with the original source identifier only. This identifier was used to track all sample handling, tasks, results etc. The samples (and all derived aliquots) were tracked by the LIMS system. All portions of any sample were automatically assigned their own unique identifiers by the LIMS when a new task is created; the relationship of these samples is also tracked. All samples were maintained at −80° C until processed.

Sample preparation—Samples were prepared using the automated MicroLab STAR® system from Hamilton Company. A recovery standard was added prior to the first step in the extraction process for QC purposes. Sample preparation was conducted using aqueous methanol extraction process to remove the protein fraction while allowing maximum recovery of small molecules. The resulting extract was divided into four fractions: one for analysis by UPLC/MS/MS (positive mode), one for UPLC/MS/MS (negative mode), one for GC/MS, and one for backup. Samples were placed briefly on a TurboVap® (Zymark) to remove the organic solvent. Each sample was then frozen and dried under vacuum. Samples were then prepared for the appropriate instrument, either UPLC/MS/MS or GC/MS.

Ultrahigh performance liquid chromatography/Mass Spectroscopy (UPLC/MS/MS)—The LC/MS portion of the platform was based on a Waters ACQUITY ultra-performance liquid chromatography (UPLC) and a Thermo-Finnigan linear trap quadrupole (LTQ) mass spectrometer, which consisted of an electrospray ionization (ESI) source and linear ion-trap (LIT) mass analyzer. The sample extract was dried then reconstituted in acidic or basic LC-compatible solvents, each of which contained 8 or more injection standards at fixed concentrations to ensure injection and chromatographic consistency. One aliquot was analyzed using acidic positive ion optimized conditions and the other using basic negative ion optimized conditions in two independent injections using separate dedicated columns. Extracts reconstituted in acidic conditions were gradient eluted using water and methanol containing 0.1% formic acid, while the basic extracts, which also used water/methanol, contained 6.5 mM Ammonium Bicarbonate. The MS analysis alternated between MS and data-dependent MS2 scans using dynamic exclusion. Raw data files are archived and extracted as described below.

Gas chromatography/Mass Spectroscopy (GC/MS)—The samples destined for GC/MS analysis were re-dried under vacuum desiccation for a minimum of 24 hours prior to being derivatized under dried nitrogen using bistrimethyl-silyltriflouroacetamide(BSTFA). The GC column was 5% phenyl and the temperature ramp was from 40° to 300°C in a 16 minute period. Samples were analyzed on a Thermo-Finnigan Trace DSQ fast-scanning single-quadrupole mass spectrometer using electron impact ionization. The instrument was tuned and calibrated for mass resolution and mass accuracy on a daily basis. The information output from the raw data files was automatically extracted as discussed below.

Quality assurance/QC—For QA/QC purposes, additional samples were included with each day's analysis. These samples included extracts of a pool of well-characterized human plasma, extracts of a pool created from a small aliquot of the experimental samples, and process blanks. QC samples were spaced evenly among the injections and all experimental samples were randomly distributed throughout the run. A selection of QC compounds was added to every sample for chromatographic alignment, including those under test. These compounds were carefully chosen so as not to interfere with the measurement of the endogenous compounds.

Data extraction and compound identification—Raw data were extracted, peak-identified and QC processed using Metabolon's hardware and software. These systems are built on a web-service platform utilizing Microsoft's NET technologies, which run on high-performance application servers and fiber-channel storage arrays in clusters to provide active failover and load-balancing [30]. Compounds were identified by comparison to library entries of purified standards or recurrent unknown entities. Metabolon maintains a library based on authenticated standards that contains the retention time/index (RI), mass to charge ratio (*m/z*), and chromatographic data (including MS/MS spectral data) on all molecules present in the library. Furthermore, biochemical identifications are based on three criteria: retention index within a narrow RI window of the proposed identification, nominal mass match to the library ± 0.2 amu, and the MS/MS forward and reverse scores between the experimental data and authentic standards. The MS/MS scores are based on a comparison of the ions present in the experimental spectrum to the ions present in the library spectrum. While there may be similarities between these molecules based on one of these factors, the use of all three data points can be utilized to distinguish and differentiate biochemicals. More than 2400 commercially available purified standard compounds have been acquired and registered into LIMS for distribution to both the LC and GC platforms for determination of their analytical characteristics.

Statistical calculation—Metabolites with missing intensity scores, indicating low levels of the metabolite in the sample, were imputed with a small number (half of the minimum value for the study). Principal component analysis was used to detect outlying samples. PLS-DA was used for assessment of separability of the samples. T-tests, allowing unequal variance, were used to compare changes in mean expression per metabolite between the control and disease groups. Boxplots of t-statistics depict changes in metabolites of similar molecule type or function. Those with $p<0.05$ were included in a heat map using metabolite-level normalized data. Samples were clustered by complete linkage on Pearson's correlation, rows are ordered by direction of change and then molecule type. Boxplots of metabolite intensity per group were also drawn for each significantly changed metabolite. A z-score plot was drawn with the z-scores based on the mean and standard deviation of the control samples per metabolite. KEGG pathway analysis (http://www.genome.jp/kegg) of 80 Homo sapiens associated pathways considered both statistical enrichment of changed intensity using the GlobalTest [31] and the impact of metabolite changes based on the pathway topology using the relative betweeness centrality measure [32]. Metabolites were mapped to the KEGG pathways using Human Metabolome Databse (HMDB; www.hmdb.ca/) number; n=228 were retained. Statistical analyses were conducted with "R" http://cran.r-project.org/, except for the PCA, PLS-DA, and pathway analysis which were conducted with "MetaboAnalyst 2.0" (http://www.metaboanalyst.ca/ [33,34]) and using log-transformed data.

Results and Discussion

Characterization of the clinical pathological state of EAE in SJL mice

The goal of this study was to profile the metabolic changes in plasma associated with clinical pathological state in experimental autoimmune encephalitis (EAE), a well-characterized animal model of multiple sclerosis (MS). For this, we induced EAE in SJL mice using $PLP_{139-151}$ peptide as described before [24]. Mice exhibited two episodes of relapsing and remitting, followed by the chronic phase of the disease (Figure 1A). At the chronic phase of disease (day 45), plasma was isolated for metabolomic profile and the spinal cords were collected and processed for CNS pathology recording inflammation, demyelination and axonal loss. The lymph nodes (LN) were processed for recall response to identify the relationship between altered metabolic changes, clinical pathology and immune response in SJL mice with EAE. Pathological analysis of CNS tissue showed that EAE group displayed inflammation and demyelination, as expected (Figures 1B and 1C). We further counted the absolute number of axons in the normal-appearing white matter at T6 which provided a global representation of the axon loss from multiple, randomly distributed demyelinated lesions throughout the spinal cord. There were 26% fewer axons in untreated EAE group compared to the healthy group ($p<0.001$) (Figure 1D). On performing recall response using LN cells, we observed production of pro-inflammatory cytokines (IFNγ and IL17) (Figure 1E). Overall, these set of data characterize the clinical and pathological state of EAE in SJL mice obtained at day 45 of disease induction.

Alteration of metabolites in plasma of EAE mice are linked to various metabolic pathways

In search of circulating metabolites as biomarkers of EAE disease, we profiled the global metabolome using liquid and gas chromatography coupled with mass spectrometry to identify the relative levels of metabolites in plasma of EAE diseased mice versus healthy control mice. Evaluation of untargeted metabolomic profiling of plasma from EAE and healthy SJL mice detected 282 known metabolites (Supplementary Table 1). One control sample was found to be an outlier dominating the first principal component in a PCA (Supplementary Figure 1) and was excluded from further analysis. PLS-DA revealed a clear separation between EAE and healthy groups, indicating presence of unique metabolite

profiles for the EAE and healthy mice group (Figure 2A). We have depicted the EAE profile (red) relative to that of healthy mice (blue) in a Z score plot (Figure 2B), where each point represents a metabolite intensity measure (rows) normalized by the mean and standard deviation of the healthy samples. Positive points represent up-regulation whereas negative points represent down regulation of the particular metabolite in the EAE mice. Metabolites are arranged by class and then by subclass. Two-sample t-tests per metabolite identified biochemicals with significantly different average intensity between the experimental groups. We found that 44 out of the 282 (15%) metabolites were differentially altered ($P<0.05$ with FDR<0.23), indicating a robust alteration in the circulating metabolomic profile during disease. Among the perturbed metabolites, 32 were up regulated in EAE plasma whereas 12 were down regulated.

Of these 44 altered compounds, ~47% belonged to the lipid class including lysolipids, bile acids, sterols, medium/long chain fatty acids, fatty acid and fatty acid metabolism, and inositol metabolism. The rest of the compounds represent amino acids, xenobiotics, cofactor and vitamins, and carbohydrates with one nucleotide and one energy class molecule (Figure 2C, Tables 1 and 2). To visualize the relationship between the 44 altered metabolites, a heatmap was generated with the metabolites arranged on the basis of relative change (up/down) and then by super pathway and samples ordered by hierarchical clustering (Figure 2D). Though the metabolites in this heatmap were selected based on average intensity differences, it is reassuring to see that these metabolites show enough distinct changes to separate the two diagnostic groups.

The most striking alteration was observed in a system-wide increase in plasma free fatty acid (FFA) levels, predominantly in the medium-chain and long-chain fatty acids (LCFAs) in the plasma of EAE group (Figure 3A). The increase in FFAs could be due to higher lipolysis or break down of membrane lipids. Lipolysis from adipose tissue and liver could also potentially be a significant source for the observed increase in plasma FFA levels. Our interpretation of higher lipolysis due to adipose tissue is supported by a recent metabolic flexibility study in MS patients, where higher lipolytic activity in adipose tissue was observed in MS patients compared to healthy [35]. Although no significant change was found in choline levels in plasma of the EAE group compared to healthy, a decreasing trend was observed. Presently, we do not have an explanation for this observation as choline serves several cellular functions including being the major head group for membrane lipid (phosphatidylcholine) especially the myelin sheath. The levels of many detected lysolipids increased with EAE disease, suggesting a possible increase in membrane breakdown and offering one possible scenario for the observed increase in the plasma FFA. The role of phospholipases in MS and EAE is well documented and they have been shown to be elevated during disease [36,37]. An elevated level of myo-inositol (MI) was found in EAE which is an organic osmolyte and a purported glial marker [38]. Changes in MI levels have been associated with onset of cognitive decline in neuroinflammatory conditions including MS [39,40]. Disease induction was also associated with changes in glycolysis (3-phosphoglycerate), TCA (alpha-ketogluterate) and glycemic control (higher levels of 1,2-AG) and histidine metabolism (Figures 3D,3F and 5). Primarily, EAE disease induction brought a system-wide increase in FFA levels. The increase in plasma FFA levels could result from multiple processes including but not limited to lipolysis, membrane breakdown and dietary uptake. Without supporting information from other tissues, it is difficult to pinpoint the source(s) of this observed increase in plasma FFAs.

Acylcarnitines, a marker of incomplete fatty acid β-oxidation, have been reported in metabolic disorders including diabetes, cardiovascular and mitochondrial diseases, were also elevated in EAE plasma [41,42]. In animal models of metabolic disorders, its increased levels have been linked to mitochondrial overload under metabolic stress [43,44]. Recent

studies are implicating mitochondrial dysfunction as one of the causes of axonal dysfunction in MS [45,46].

We found elevated levels of various metabolites categorized under xenobiotics class (Figure 3B), which are normally not synthesized in the body, but can be metabolized by the micro-biome of the distal gut, and their elevated levels can be observed in biological fluids under normal or pathological state. The most dramatically increased xenobiotic metabolites observed in the plasma of EAE were equolsulphate and homostachydrine. While, no biological role has been identified for these two metabolites, a recent study reported that equolsulphate was observed in the plasma of conventional mice but not in the plasma of germ-free mice [47], suggesting a significant interplay between resident bacterial and mammalian metabolism. Homostachydrine has been reported in citrus genus plants [48], but with no biological activity defined. Stachydrine was significantly elevated in plasma of EAE, which was recently shown to activate Th17/Th1 by reducing Th2/Treg in RU486 induced mouse model [49]. This observation agrees with the identified higher levels of stachydrine, increased inflammation and severity in SJL mice with EAE (Figure 1). Benzoate (benzoic acid) a monocarboxylate, is used as a food preservative and is also used for the treatment of hyperammonemia [50]. It has been shown to have anti-inflammatory properties, and reduced microglial and astroglial inflammatory responses and EAE disease progression [51,52]. Its metabolism occurs exclusively by conjugation with glycine to form hippurate. It is a mammalian-microbial co-metabolite and a normal constituent of the endogenous urinary metabolite profile. Its excretion has been reported in various disease conditions including normal constituent of the endogenous urinary metabolite profile. Its excretion has been reported in various disease conditions including obesity, diabetes, gastrointestinal diseases, impaired renal function and psychological disorders [53]. We observed significantly higher level of both benzoate and hippurate in the plasma of EAE afflicted mice. Strong evidence for the pivotal role of the gut microbiota in the generation of hippurate [54] further suggesting the alteration of gut microbiome during disease, which may be responsible for altered levels of xenobiotics in plasma of EAE group. Indoleacrylate (indoleacrylic acid; IAcrA), a metabolite of tryptophan pathway, is highly reactive and conjugates with glycine to form indolylacryloylglycine (IAG), which is excreted in urine. The only significantly decreased xenobiotic found in EAE plasma was glycolate (glycolic acid), which is considered a major precursor of oxalate in hepatocytes.

We observed elevated levels of two metabolites, alpha-tocopherol (vitamin E) and salicylate in plasma (Figures 3B and 3E), known to have anti-inflammatory and protective effect against inflammation. Alpha-tocopherol exhibits anti-oxidant and anti-inflammatory properties. Alpha-tocopherol was shown to be significantly increased during clinical attack in EAE [55], however, its levels were found to be reduced in MS patients [56], which is dissimilar from our finding. Salicylate is a well known inhibitor of cyclooxygenase and has been shown to attenuate EAE disease progression and inflammation [57]. Trigoneline, an alkaloid and coffee constituent, was elevated in the plasma of EAE (Figure 3E). It has been reported to have anti-diabetic property [58]. Higher levels of these compounds found in the plasma of EAE could be a self-protective mechanism up regulated during disease against the inflammatory cascades.

To get a holistic view of the metabolic alterations occurring in the plasma of EAE mice we conducted pathway analysis of the biochemical pathways of the Kyoto Encyclopedia of Genes and Genomics (KEGG, http://genome.jp/kegg). We considered both concerted changes in metabolite intensity within the pathway (GlobalTest) [31] and alterations of high impact (i.e. at major junctions in the pathway), and found that a number of pathways were significantly altered (Figure 4A). We selected six pathways based on p values and high impact factor (Figure 4B). Pathways found to be altered based on the Global Test included

primary bile acid biosynthesis, taurine and hypotaurine metabolism, tryptophan and histidine metabolism. Linoleic acid and D-arginine and D-orinithine metabolism pathways had altered metabolites with high impact. These pathways are highly integrated as shown in Figure 5, suggesting that perturbation of certain central metabolites could have impact on multiple metabolic pathways. While some of these metabolite changes could easily be developed as biomarkers of the disease, the key to translating metabolomics into therapeutics would require figuring out the central altered metabolic pathway(s).

Major pathways with concerted alterations during EAE disease

Primary bile acid biosynthesis metabolism—Bile acids are steroids found predominately in the bile of mammals and their main function is to facilitate the formation of micelles to promote processing of fat. Both primary and secondary circulatory bile acid levels (Deoxycholate, Taurodeoxycholate and alpha-muricholate) were decreased in the EAE group, which could either be due to a more efficient uptake of bile acids from enterohepatic circulation or decreased synthesis in the liver. Bile acid precursor, cholesterol was found to be increased during disease, which is a known risk factor for several diseases including atherosclerosis, possibly suggesting a decrease in hepatic bile acid synthesis. Alternatively, it could also indicate an increase in cholesterol synthesis in response to EAE disease. Changes in bile acid levels could affect dietary lipid absorption. Increase in cholesterol levels in plasma in EAE has been previously reported [59], however, no conclusive reports are available indicating a relationship between higher cholesterol and MS incidence in patients. Under normal conditions, the most abundant bile acids are chenodeoxycholic acid (45%) and cholic acid (31%), referred to as primary bile acids. Before they are secreted from lumen, they are conjugated with amino acids glycine or taurine and called glycoconjugates and tauroconjugates, respectively. In human and rat, both conjugates are present, however, in mouse, only tauroconjugates are formed. We found decreased levels of deoxycholate in plasma, which may reflect that gut bacteria may be not able to efficiently modify primary bile acids (cholate) into secondary bile acids (deoxycholate). Decreased level of deoxycholate is reflected in lower levels of taurocdeoxycholate observed in diseased mice (Figures 3A and 5). Alpha-mucholic acid was also decreased in plasma of EAE group; however, taurocholic acid and taurochenodeoxycholic acids were unaffected compared to healthy group. Deoxycholic acid is reported to activate farnesoid X receptor (FXR) [60], which is a nuclear receptor controlling genes of various pathways including bile acid synthesis, cholesterol, glycolysis, glyconeogenesis and fatty acid oxidation [61]. Moreover, activation of FXR shows anti-inflammatory property in inflammatory models [62,63], raising the question whether decreased levels of anti-inflammatory bile acids could be one of the factors contributing towards the severity of disease in EAE.

Tryptophan metabolism—Tryptophan metabolism is critical for two important biosynthetic pathways; 1: generation of neurotransmitter 5-hydroxytryptamin (serotonin) by tryptophan 5-hydroxylkase, and 2: the formation of kynurenine derivatives and NAD. Serotonin is a major neurotransmitter in the enteric nervous system (ENS) as well as in CNS. A portion of serotonin is further converted to melatonin, affecting sleep pattern. Although we did not observe any changes in the levels of tryptophan and serotonin, the level of kynurenate (kynurenic acid) was significantly low in plasma of EAE, which is a metabolite of kynurenine. On the other hand, indolepropionate and indoleacrylate levels were found to be elevated in EAE, suggesting a disruption of tryptophan metabolism in EAE. Tryptophan catabolism is regulated by the balanced expression of indolamine 2,3-dioxygenase (IDO)/tryptophanyl-tRNA-synthase (TTS). IDO is expressed in a variety of cells in CNS including macrophage/activated microglia during disease [64], and drives

immune dysfunction by suppressing T cell proliferation, altering Th17/Treg balance and controlling EAE disease [8].

Taurine and hypotaurine metabolism—Taurine is a major constituent of bile and accounts for approximately 0.1% of total human body weight. Apart from the fundamental biological roles it plays in conjugation of bile acids, as an anti-oxidant, osmoregulation, membrane stabilization and calcium signaling, it also has immunomodulatory and neuroprotective effects [65]. Taurine and its metabolites inhibit T cell response and functions of antigen presenting cells, and thereby play an important role in maintaining the balance between the inflammatory response and the induction of an antigen specific immune response [66]. Our observation that taurine metabolism pathway is significantly altered is in accordance with previous published observations in EAE and MS CSF, where higher levels of taurine was also observed [23,67,68]. Our data reveals that this increase in taurine can also be determined in the plasma, without the need of CSF, and could be a potential biomarker.

Histidine metabolism—While histidine levels were found to be increased, one of its metabolites (also an antioxidant), anserine, showed a decreasing trend in the EAE group. Histamine, one of the metabolites in histidine metabolism, has been shown to play regulatory role in EAE by altering the permeability of the BBB and promoting CNS inflammation [69,70]. Its levels were reported to be significantly higher in CSF of MS patients [71]. Changes in histidine metabolism could potentially affect histamine levels.The biosynthesis of histidine is inherently linked to the nucleotide pathway through 5-phosphoribosyl-1-pyrophsophate (PRPP) [72]. Circulatory nucleosides including N4-acetylcytidine were increased in EAE group compared to healthy group, possibly being generated from the increased degradation of synthesized RNA [73]. Anserine, which was significantly decreased in EAE plasma, is a di-peptide of beta-alanine and N-methyl-histidine. It is an anti-oxidant found in skeletal muscle and brain, and inhibits the catalysis of lipid oxidation. Another antioxidant, alpha-tocopherol was increased during EAE disease while no change was found in metabolites involved in the glutathione pathway. It is accepted that a critical balance between various anti-oxidants could tilt the severity of disease in EAE.

Major pathways affected by alterations of high impact molecules during EAE disease

Linoleic acid metabolism—Linoleic acid (LA) is a member of the essential fatty acids called omega-6 fatty acids. LA is a precursor of eicosanoids, which have pro- and anti-inflammatory effect in vitro and in vivo. Its levels were found to be low in MS patients [74,75], suggesting the perturbation of this pathway during disease. Clinical trials in MS patients revealed that treatment with LA reduced the severity and duration of relapses at all levels of disability and duration of illness at entry to the trials [76]. Recently, a randomised, double-blind, placebo-controlled proof-of-concept clinical trial using novel oral nutraceutical formula of omega-3 and omega-6 fatty acids with vitamins (PLP10) in relapsing remitting multiple sclerosis showed a significant reduction in annualized relapse rate and the risk of sustained disability progression without any reported serious adverse events [77]. Moreover, oral feeding of LA has been reported to attenuate EAE disease progression associated with an increase in cell membrane long chain omega-6 fatty acids, production of prostaglandin E2 (PGE2) and the expression of TGFβ1 in mice [78] and guinea pigs [79]. Omega-3 and omega-6 PUFAs modulate transcription via interactions with peroxisome proliferator-activated receptors (PPARs), which increase fatty acid oxidation and suppress lipogenesis and control inflammation by repressing various transcription factors including NFκB, NFAT, AP-1 and STATs [80,81]. These reports support that

linoleic metabolism pathway is affected during EAE/MS disease and restoring omega-6 fatty acid levels may have beneficial effect in EAE and MS patients.

D-Arginine and D-ornithine pathway—This pathway described the general conversion of D-amino acids to oxo-amino acids by D-amino acid oxidase. D-amino acids can be found in some bacteria or may spontaneously form via isomerase/mutase reactions. D-arginine converted to L-arginine, which is the main substrate for nitric oxide (NO) synthesis during inflammation in EAE and MS. Overexpression of iNOS in the infiltrated macrophages and resident microglia/astrocytes leads to intense production of NO in the CNS [82]. The role of NO in EAE and MS is elusive. Although arginine level was not altered in plasma in EAE, citrulline levels were decreased significantly. Citrullline can be derived from multiple sources including from arginine via NOS or from ornithine via catabolism of proline and glutamine/glutamate. During inflammation in EAE, NOS in immune cells used arginine as a substrate producing NO as aninflammatory mediator and citrulline as a byproduct. In contrast, citrulline levels were significantly low in plasma during EAE. The most plausible explanation is that citrulline is extracted from circulation by proximal tubules of kidney, converted to arginine and returned to circulation, resulting in unaffected arginine levels in plasma of EAE.

Conclusions

Altogether, using untargeted metabolomics profiling, this study provides a better understanding of metabolic abnormalities in RR EAE mouse model at chronic phase of the disease. We identified 44 metabolite signature discriminating EAE from the healthy group that correlated with the clinical pathology of the disease. These metabolites pertaining to six identified pathways are highly integrated and participate in anti- and pro-inflammatory responses in body (Figure 5). Balance between these pathways possibly decides the outcome of the disease. We do realize that by limiting analysis to one time point, we may have missed earlier metabolic changes that may serve as early biomarker(s) in the mouse model. Earlier time points and other tissues will be subjected to metabolic profiling in the future to provide more insights into the mechanisms related to EAE disease. We appreciate that the in depth mechanistic studies with specific metabolite(s) and/or pathways are required to judge the true contribution or effect on the disease process. However, we believe this is the first step in appreciating the milieu of metabolic changes associated with the EAE/MS disease process. In conclusion, the plasma metabolomics possesses great potential in biomarker discovery and in investigation of the underlying metabolic mechanisms for EAE/MS. Moreover, these findings clearly suggest that creation of new treatment paradigms targeting and modulating these metabolic pathways in their entirety, rather than single protein or pathway (for example immunomodulation), might be necessary for controlling and treating demyelinating disease in humans.

Supplementary Material

Refer to Web version on PubMed Central for supplementary material.

Acknowledgments

This investigation was mainly supported by grants (RG3810-A-1 and RG4311A4/4) from the National Multiple Sclerosis Society and 5R21NS65928 NIH to SG.

Abbreviations

EAE	Experimental Autoimmune Encephalitis
MS	Multiple Sclerosis
CNS	Central Nervous System
RR	Relapsing Remitting
FDR	False Discovery Rate
KEGG	Kyoto Encyclopedia of Genes and Genomics
MBP	Myelin Basic Protein
MOG	Myelin Oligodendrocyte Glycoprotein
PLP	Proteolipod Protein
CFA	Complete Freund's Adjuvant
Th	T Helper
TNFa	Tumor Necrosis Factor Alpha
IL	Interleukin
BBB	Blood Brain Barrier
IDO	Indoleamine 2,3-Dioxygenase
UPLC/MS/MS	Ultrahigh Performance Liquid Chromatography/Mass Spectroscopy
GC/MS	Gas Chromatography/Mass Spectroscopy
PCA	Principal Component Analysis
FFA	Free Fatty Acid
LCFAs	Long-Chain Fatty Acids
Iacra	Indoleacrylic Acid
FXR	Farnesoid X Receptor
PGE2	Prostaglandin E2
PPARs	Peroxisome Proliferator-Activated Receptors
LA	Linoleic Acid
NO	Nitric Oxide
PLS-DA	Partial Least Squares Discriminant Analysis

References

1. Gold R, Hartung HP, Toyka KV. Animal models for autoimmune demyelinating disorders of the nervous system. Mol Med Today. 2000; 6:88–91. [PubMed: 10652482]
2. Martin R, McFarland HF, McFarlin DE. Immunological aspects of demyelinating diseases. Annu Rev Immunol. 1992; 10:153–187. [PubMed: 1375472]
3. Swanborg RH. Experimental autoimmune encephalomyelitis in the rat: lessons in T-cell immunology and autoreactivity. Immunol Rev. 2001; 184:129–135. [PubMed: 12086308]
4. Ando DG, Clayton J, Kono D, Urban JL, Sercarz EE. Encephalitogenic T cells in the B10.PL model of experimental allergic encephalomyelitis (EAE) are of the Th-1 lymphokine subtype. Cell Immunol. 1989; 124:132–143. [PubMed: 2478300]

5. Kuchroo VK, Anderson AC, Waldner H, Munder M, Bettelli E, et al. T cell response in experimental autoimmune encephalomyelitis (EAE): role of self and cross-reactive antigens in shaping, tuning, and regulating the autopathogenic T cell repertoire. Annu Rev Immunol. 2002; 20:101–123. [PubMed: 11861599]
6. Zamvil SS, Steinman L. The T lymphocyte in experimental allergic encephalomyelitis. Annu Rev Immunol. 1990; 8:579–621. [PubMed: 2188675]
7. Korn T, Bettelli E, Oukka M, Kuchroo VK. IL-17 and Th17 Cells. Annu Rev Immunol. 2009; 27:485–517. [PubMed: 19132915]
8. Yan Y, Zhang GX, Gran B, Fallarino F, Yu S, et al. IDO upregulates regulatory T cells via tryptophan catabolite and suppresses encephalitogenic T cell responses in experimental autoimmune encephalomyelitis. J Immunol. 2010; 185:5953–5961. [PubMed: 20944000]
9. Gerriets VA, Rathmell JC. Metabolic pathways in T cell fate and function. Trends Immunol. 2012; 33:168–173. [PubMed: 22342741]
10. Mellor AL, Munn DH. Tryptophan catabolism and T-cell tolerance: immunosuppression by starvation? Immunol Today. 1999; 20:469–473. [PubMed: 10500295]
11. Viollet B, Horman S, Leclerc J, Lantier L, Foretz M, et al. AMPK inhibition in health and disease. Crit Rev Biochem Mol Biol. 2010; 45:276–295. [PubMed: 20522000]
12. Nicholson JK, Lindon JC. Systems biology: Metabonomics. Nature. 2008; 455:1054–1056. [PubMed: 18948945]
13. Zhang AH, Sun H, Wang XJ. Recent advances in metabolomics in neurological disease, and future perspectives. Anal Bioanal Chem. 2013
14. Johnson CH, Gonzalez FJ. Challenges and opportunities of metabolomics. J Cell Physiol. 2012; 227:2975–2981. [PubMed: 22034100]
15. Mamas M, Dunn WB, Neyses L, Goodacre R. The role of metabolites and metabolomics in clinically applicable biomarkers of disease. Arch Toxicol. 2011; 85:5–17. [PubMed: 20953584]
16. Corona G, Rizzolio F, Giordano A, Toffoli G. Pharmaco-metabolomics: an emerging “omics” tool for the personalization of anticancer treatments and identification of new valuable therapeutic targets. J Cell Physiol. 2012; 227:2827–2831. [PubMed: 22105661]
17. Sreekumar A, Poisson LM, Rajendiran TM, Khan AP, Cao Q, et al. Metabolomic profiles delineate potential role for sarcosine in prostate cancer progression. Nature. 2009; 457:910–914. [PubMed: 19212411]
18. Sato Y, Suzuki I, Nakamura T, Bernier F, Aoshima K, et al. Identification of a new plasma biomarker of Alzheimer’s disease using metabolomics technology. J Lipid Res. 2012; 53:567–576. [PubMed: 22203775]
19. Trushina E, Nemutlu E, Zhang S, Christensen T, Camp J, et al. Defects in mitochondrial dynamics and metabolomic signatures of evolving energetic stress in mouse models of familial Alzheimer’s disease. PLoS One. 2012; 7:e32737. [PubMed: 22393443]
20. Johansen KK, Wang L, Aasly JO, White LR, Matson WR, et al. Metabolomic profiling in LRRK2-related Parkinson’s disease. PLoS One. 2009; 4:e7551. [PubMed: 19847307]
21. Gebregiworgis T, Massilamany C, Gangaplara A, Thulasingam S, Kolli V, et al. Potential of urinary metabolites for diagnosing multiple sclerosis. ACS Chem Biol. 2013; 8:684–690. [PubMed: 23369377]
22. Lutz NW, Fernandez C, Pellissier JF, Cozzone PJ, Béraud E. Cerebral biochemical pathways in experimental autoimmune encephalomyelitis and adjuvant arthritis: a comparative metabolomic study. PLoS One. 2013; 8:e56101. [PubMed: 23457507]
23. Noga MJ, Dane A, Shi S, Attali A, van Aken H, et al. Metabolomics of cerebrospinal fluid reveals changes in the central nervous system metabolism in a rat model of multiple sclerosis. Metabolomics. 2012; 8:253–263. [PubMed: 22448154]
24. Nath N, Khan M, Paintlia MK, Singh I, Hoda MN, et al. Metformin attenuated the autoimmune disease of the central nervous system in animal models of multiple sclerosis. J Immunol. 2009; 182:8005–8014. [PubMed: 19494326]
25. Denic A, Bieber A, Warrington A, Mishra PK, Macura S, et al. Brainstem 1H nuclear magnetic resonance (NMR) spectroscopy: marker of demyelination and repair in spinal cord. Ann Neurol. 2009; 66:559–564. [PubMed: 19816926]

26. Howe CL, Adelson JD, Rodriguez M. Absence of perforin expression confers axonal protection despite demyelination. Neurobiol Dis. 2007; 25:354–359. [PubMed: 17112732]
27. Boudonck KJ, Mitchell MW, Német L, Keresztes L, Nyska A, et al. Discovery of metabolomics biomarkers for early detection of nephrotoxicity. Toxicol Pathol. 2009; 37:280–292. [PubMed: 19380839]
28. Evans AM, DeHaven CD, Barrett T, Mitchell M, Milgram E. Integrated, nontargeted ultrahigh performance liquid chromatography/electrospray ionization tandem mass spectrometry platform for the identification and relative quantification of the small-molecule complement of biological systems. Anal Chem. 2009; 81:6656–6667. [PubMed: 19624122]
29. Lawton KA, Berger A, Mitchell M, Milgram KE, Evans AM, et al. Analysis of the adult human plasma metabolome. Pharmacogenomics. 2008; 9:383–397. [PubMed: 18384253]
30. Dehaven CD, Evans AM, Dai H, Lawton KA. Organization of GC/MS and LC/MS metabolomics data into chemical libraries. J Cheminform. 2010; 2:9. [PubMed: 20955607]
31. Goeman JJ, Bühlmann P. Analyzing gene expression data in terms of gene sets: methodological issues. Bioinformatics. 2007; 23:980–987. [PubMed: 17303618]
32. Aittokallio T, Schwikowski B. Graph-based methods for analysing networks in cell biology. Brief Bioinform. 2006; 7:243–255. [PubMed: 16880171]
33. Xia J, Mandal R, Sinelnikov IV, Broadhurst D, Wishart DS. MetaboAnalyst 2.0--a comprehensive server for metabolomic data analysis. Nucleic Acids Res. 2012; 40:W127–133. [PubMed: 22553367]
34. Xia J, Psychogios N, Young N, Wishart DS. MetaboAnalyst: a web server for metabolomic data analysis and interpretation. Nucleic Acids Res. 2009; 37:W652–660. [PubMed: 19429898]
35. Mähler A, Steiniger J, Bock M, Brandt AU, Haas V, et al. Is metabolic flexibility altered in multiple sclerosis patients? PLoS One. 2012; 7:e43675. [PubMed: 22952735]
36. Kalyvas A, Baskakis C, Magrioti V, Constantinou-Kokotou V, Stephens D, et al. Differing roles for members of the phospholipase A2 superfamily in experimental autoimmune encephalomyelitis. Brain. 2009; 132:1221–1235. [PubMed: 19218359]
37. Marusic S, Leach MW, Pelker JW, Azoitei ML, Uozumi N, et al. Cytosolic phospholipase A2 alpha-deficient mice are resistant to experimental autoimmune encephalomyelitis. J Exp Med. 2005; 202:841–851. [PubMed: 16172261]
38. Brand A, Richter-Landsberg C, Leibfritz D. Multinuclear NMR studies on the energy metabolism of glial and neuronal cells. Dev Neurosci. 1993; 15:289–298. [PubMed: 7805581]
39. Fernando KT, McLean MA, Chard DT, MacManus DG, Dalton CM, et al. Elevated white matter myo-inositol in clinically isolated syndromes suggestive of multiple sclerosis. Brain. 2004; 127:1361–1369. [PubMed: 15128615]
40. Huang W, Alexander GE, Daly EM, Shetty HU, Krasuski JS, et al. High brain myo-inositol levels in the predementia phase of Alzheimer's disease in adults with Down's syndrome: a 1H MRS study. Am J Psychiatry. 1999; 156:1879–1886. [PubMed: 10588400]
41. Adams SH, Hoppel CL, Lok KH, Zhao L, Wong SW, et al. Plasma acylcarnitine profiles suggest incomplete long-chain fatty acid beta-oxidation and altered tricarboxylic acid cycle activity in type 2 diabetic African-American women. J Nutr. 2009; 139:1073–1081. [PubMed: 19369366]
42. Sampey BP, Freemerman AJ, Zhang J, Kuan PF, Galanko JA, et al. Metabolomic profiling reveals mitochondrial-derived lipid biomarkers that drive obesity-associated inflammation. PLoS One. 2012; 7:e38812. [PubMed: 22701716]
43. Koves TR, Ussher JR, Noland RC, Slentz D, Mosedale M, et al. Mitochondrial overload and incomplete fatty acid oxidation contribute to skeletal muscle insulin resistance. Cell Metab. 2008; 7:45–56. [PubMed: 18177724]
44. Noland RC, Koves TR, Seiler SE, Lum H, Lust RM, et al. Carnitine insufficiency caused by aging and overnutrition compromises mitochondrial performance and metabolic control. J Biol Chem. 2009; 284:22840–22852. [PubMed: 19553674]
45. Dutta R, McDonough J, Yin X, Peterson J, Chang A, et al. Mitochondrial dysfunction as a cause of axonal degeneration in multiple sclerosis patients. Ann Neurol. 2006; 59:478–489. [PubMed: 16392116]

46. Mahad DJ, Ziabreva I, Campbell G, Lax N, White K, et al. Mitochondrial changes within axons in multiple sclerosis. Brain. 2009; 132:1161–1174. [PubMed: 19293237]
47. Wikoff WR, Anfora AT, Liu J, Schultz PG, Lesley SA, et al. Metabolomics analysis reveals large effects of gut microflora on mammalian blood metabolites. Proc Natl Acad Sci U S A. 2009; 106:3698–3703. [PubMed: 19234110]
48. Servillo L, Giovane A, Balestrieri ML, Ferrari G, Cautela D, et al. Occurrence of pipecolic acid and pipecolic acid betaine (homostachydrine) in Citrus genus plants. J Agric Food Chem. 2012; 60:315–321. [PubMed: 22208890]
49. Li X, Wang B, Li Y, Wang L, Zhao X, et al. The Th1/Th2/Th17/Treg paradigm induced by stachydrine hydrochloride reduces uterine bleeding in RU486-induced abortion mice. J Ethnopharmacol. 2013; 145:241–253. [PubMed: 23178269]
50. Brusilow SW, Danney M, Waber LJ, Batshaw M, Burton B, et al. Treatment of episodic hyperammonemia in children with inborn errors of urea synthesis. N Engl J Med. 1984; 310:1630–1634. [PubMed: 6427608]
51. Brahmachari S, Jana A, Pahan K. Sodium benzoate, a metabolite of cinnamon and a food additive, reduces microglial and astroglial inflammatory responses. J Immunol. 2009; 183:5917–5927. [PubMed: 19812204]
52. Brahmachari S, Pahan K. Sodium benzoate, a food additive and a metabolite of cinnamon, modifies T cells at multiple steps and inhibits adoptive transfer of experimental allergic encephalomyelitis. J Immunol. 2007; 179:275–283. [PubMed: 17579047]
53. Lees HJ, Swann JR, Wilson ID, Nicholson JK, Holmes E. Hippurate: The Natural History of a Mammalian-Microbial Cometabolite. J Proteome Res. 2013
54. Nicholls AW, Mortishire-Smith RJ, Nicholson JK. NMR spectroscopic-based metabonomic studies of urinary metabolite variation in acclimatizing germ-free rats. Chem Res Toxicol. 2003; 16:1395–1404. [PubMed: 14615964]
55. Honegger CG, Krenger W, Langemann H. Measurement of free radical scavengers in the spinal cord of rats with experimental autoimmune encephalomyelitis. Neurosci Lett. 1989; 98:327–332. [PubMed: 2786169]
56. Besler HT, Comoglu S, Okcu Z. Serum levels of antioxidant vitamins and lipid peroxidation in multiple sclerosis. Nutr Neurosci. 2002; 5:215–220. [PubMed: 12041878]
57. Moon C, Ahn M, Jee Y, Heo S, Kim S, et al. Sodium salicylate-induced amelioration of experimental autoimmune encephalomyelitis in Lewis rats is associated with the suppression of inducible nitric oxide synthase and cyclooxygenases. Neurosci Lett. 2004; 356:123–126. [PubMed: 14746879]
58. Zhou J, Chan L, Zhou S. Trigonelline: a plant alkaloid with therapeutic potential for diabetes and central nervous system disease. Curr Med Chem. 2012; 19:3523–3531. [PubMed: 22680628]
59. Shore VG, Smith ME, Perret V, Laskaris MA. Alterations in plasma lipoproteins and apolipoproteins in experimental allergic encephalomyelitis. J Lipid Res. 1987; 28:119–129. [PubMed: 3494804]
60. Lew JL, Zhao A, Yu J, Huang L, De Pedro N, et al. The farnesoid X receptor controls gene expression in a ligand- and promoter-selective fashion. J Biol Chem. 2004; 279:8856–8861. [PubMed: 14684751]
61. Lefebvre P, Cariou B, Lien F, Kuipers F, Staels B. Role of bile acids and bile acid receptors in metabolic regulation. Physiol Rev. 2009; 89:147–191. [PubMed: 19126757]
62. Gadaleta RM, van Erpecum KJ, Oldenburg B, Willemsen EC, Renooij W, et al. Farnesoid X receptor activation inhibits inflammation and preserves the intestinal barrier in inflammatory bowel disease. Gut. 2011; 60:463–472. [PubMed: 21242261]
63. Zhang L, Li T, Yu D, Forman BM, Huang W. FXR protects lung from lipopolysaccharide-induced acute injury. Mol Endocrinol. 2012; 26:27–36. [PubMed: 22135065]
64. Kwidzinski E, Bunse J, Aktas O, Richter D, Mutlu L, et al. Indolamine 2,3-dioxygenase is expressed in the CNS and down-regulates autoimmune inflammation. FASEB J. 2005; 19:1347–1349. [PubMed: 15939737]

65. Sternberg Z, Cesario A, Rittenhouse-Olson K, Sobel RA, Leung YK, et al. Acamprosate modulates experimental autoimmune encephalomyelitis. Inflammopharmacology. 2012; 20:39–48. [PubMed: 22090150]
66. Marcinkiewicz J, Nowak B, Grabowska A, Bobek M, Petrovska L, et al. Regulation of murine dendritic cell functions in vitro by taurine chloramine, a major product of the neutrophil myeloperoxidase-halide system. Immunology. 1999; 98:371–378. [PubMed: 10583596]
67. Gårseth M, White LR, Aasly J. Little change in cerebrospinal fluid amino acids in subtypes of multiple sclerosis compared with acute polyradiculoneuropathy. Neurochem Int. 2001; 39:111–115. [PubMed: 11408089]
68. Musgrave T, Tenorio G, Rauw G, Baker GB, Kerr BJ. Tissue concentration changes of amino acids and biogenic amines in the central nervous system of mice with experimental autoimmune encephalomyelitis (EAE). Neurochem Int. 2011; 59:28–38. [PubMed: 21672584]
69. Lu C, Diehl SA, Noubade R, Ledoux J, Nelson MT, et al. Endothelial histamine H1 receptor signaling reduces blood-brain barrier permeability and susceptibility to autoimmune encephalomyelitis. Proc Natl Acad Sci U S A. 2010; 107:18967–18972. [PubMed: 20956310]
70. Orr EL, Stanley NC. Brain and spinal cord levels of histamine in Lewis rats with acute experimental autoimmune encephalomyelitis. J Neurochem. 1989; 53:111–118. [PubMed: 2786054]
71. Kallweit U, Aritake K, Bassetti CL, Blumenthal S, Hayaishi O, et al. Elevated CSF histamine levels in multiple sclerosis patients. Fluids Barriers CNS. 2013; 10:19. [PubMed: 23659456]
72. Frolkis A, Knox C, Lim E, Jewison T, Law V, et al. SMPDB: The Small Molecule Pathway Database. Nucleic Acids Res. 2010; 38:D480–487. [PubMed: 19948758]
73. Schram KH. Urinary nucleosides. Mass Spectrom Rev. 1998; 17:131–251. [PubMed: 10095827]
74. Holman RT, Johnson SB, Kokmen E. Deficiencies of polyunsaturated fatty acids and replacement by nonessential fatty acids in plasma lipids in multiple sclerosis. Proc Natl Acad Sci U S A. 1989; 86:4720–4724. [PubMed: 2734316]
75. Gul S, Smith AD, Thompson RH, Wright HP, Zilkha KJ. Fatty acid composition of phospholipids from platelets and erythrocytes in multiple sclerosis. J Neurol Neurosurg Psychiatry. 1970; 33:506–510. [PubMed: 5505678]
76. Dworkin RH, Bates D, Millar JH, Paty DW. Linoleic acid and multiple sclerosis: a reanalysis of three double-blind trials. Neurology. 1984; 34:1441–1445. [PubMed: 6387534]
77. Pantzaris MC, Loukaides GN, Ntzani EE, Patrikios IS. A novel oral nutraceutical formula of omega-3 and omega-6 fatty acids with vitamins (PLP10) in relapsing remitting multiple sclerosis: a randomised, double-blind, placebo-controlled proof-of-concept clinical trial. BMJ Open. 2013:3.
78. Harbige LS, Layward L, Morris-Downes MM, Dumonde DC, Amor S. The protective effects of omega-6 fatty acids in experimental autoimmune encephalomyelitis (EAE) in relation to transforming growth factor-beta 1 (TGF-beta1) up-regulation and increased prostaglandin E2 (PGE2) production. Clin Exp Immunol. 2000; 122:445–452. [PubMed: 11122253]
79. Hughes D, Keith AB, Mertin J, Caspary EA. Linoleic acid therapy in severe experimental allergic encephalomyelitis in the guinea-pig: suppression by continuous treatment. Clin Exp Immunol. 1980; 40:523–531. [PubMed: 7418264]
80. Bensinger SJ, Tontonoz P. Integration of metabolism and inflammation by lipid-activated nuclear receptors. Nature. 2008; 454:470–477. [PubMed: 18650918]
81. Wagner M, Zollner G, Trauner M. Nuclear receptors in liver disease. Hepatology. 2011; 53:1023–1034. [PubMed: 21319202]
82. Saha RN, Pahan K. Regulation of inducible nitric oxide synthase gene in glial cells. Antioxid Redox Signal. 2006; 8:929–947. [PubMed: 16771683]

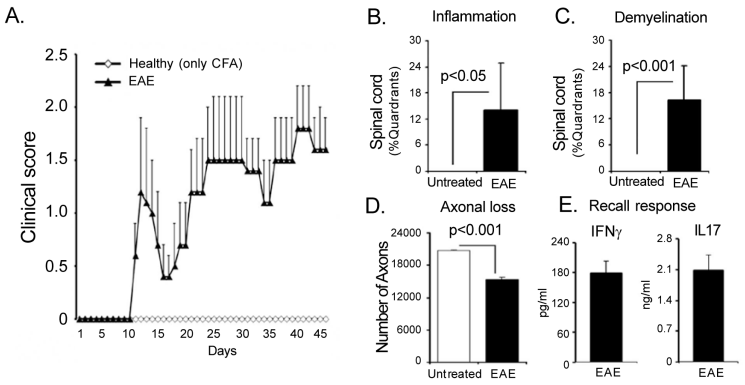

Figure 1. Characterization of clinical pathological state of EAE in RR mouse model

A. EAE was induced in SJL mice using $PLP_{139-151}$ peptide emulsified in CFA and clinical score was recorded daily (n=10). The healthy group was given CFA without peptide. Arrow represents the day when tissues/plasma were harvested for analysis. **B-C.** Percentage of spinal cord quadrants containing spinal cord white matter inflammation and demyelination (mean ± SD; n=5). **D.** Absolute number of axons counted in six areas of a mid-thoracic spinal cord section. P<0.01 and P<0.001 compared to healthy group. **E.** Recall response in cells isolated from lymph nodes, stimulated with 20 μg of $PLP_{139-151}$ for 72 h. Cell supernatant was used for measuring the levels of IFNγ and IL17 by ELISA (n=4).

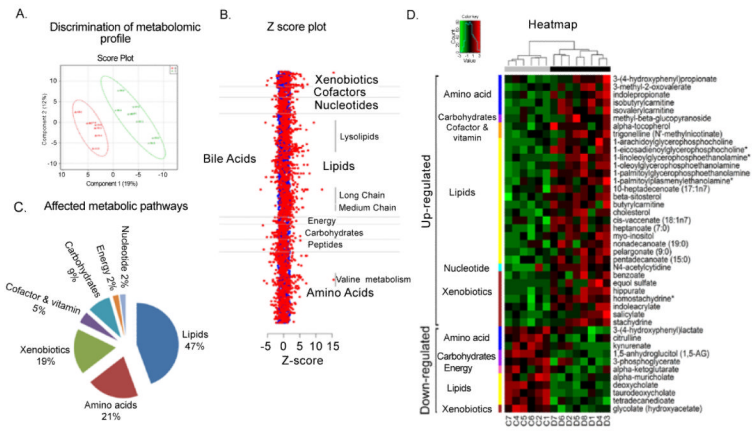

Figure 2. Metabolomics profiling of plasma distinguishes EAE from healthy group

A. Partial least squares discriminant analysis (PLS-DA) score plot of the metabolic profile of plasma isolated from the EAE and healthy groups shows clear separation. This indicates different metabolic profiles of the plasma extricates in the groups. **B.** Pie chart of the percentage of changed metabolites by major metabolic super-pathway. **C.** Z-score plot of the changed metabolites in plasma of EAE (red) compared to healthy group (blue). **D.** A heatmap drawn with the altered metabolites ($P<0.05$ with $FDR<0.23$) arranged on the basis relative change (up/down) and then by super pathway. C: control healthy; D: EAE diseased mice. Samples are ordered by hierarchical clustering. Red and green indicate increased and decreased levels, respectively.

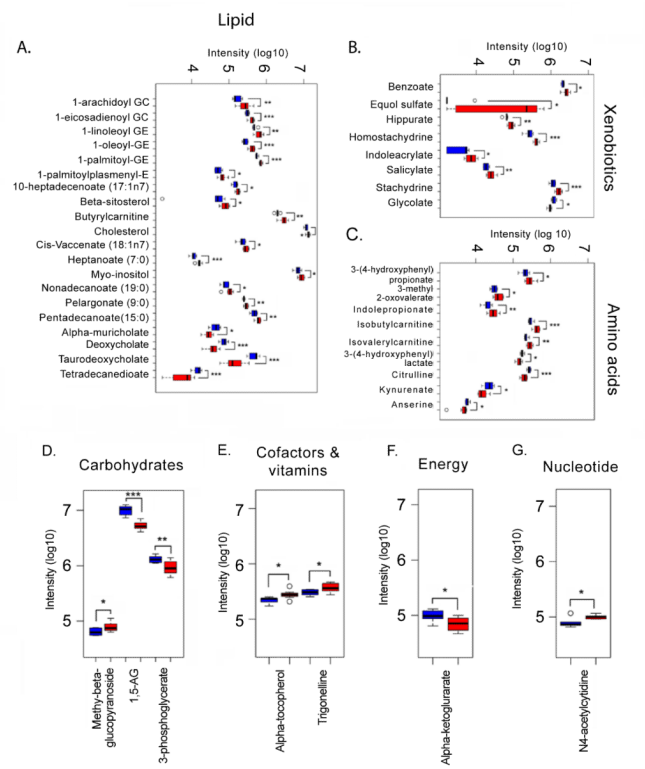

Figure 3. Box plots of various metabolite classes altered in EAE

Significantly altered metabolite intensities are shown as box plots grouped by class: lipid (i), xenobiotics (ii), amino acids (iii), carbohydrates (iv), cofactors and vitamins (v), energy (vi) and nucleotide (vii). Medians are represented by horizontal bars, boxes span the interquartile range (IQR) and whiskers extend to extreme data points within 1.5 times IQR. Outliers plotted as open circles lie outside 1.5 times the IQR. Blue and red box plots represent healthy and EAE group, respectively. *P<0.05; **P<0.01; ***P<0.001 compared to healthy group. Abbreviation used for following lysolipids: 1-arachidoyl GC: 1--arachidoylglycerophosphocholine; 1-eicosadienoyl GC: 1-eicosadienoylglycerophosphocholine; 1-linoleoyl GE: 1-linoleoylglycerophosphoethanolamine; 1-oleoyl GE: 1-oleoylglycerophosphoethanolamine; 1-palmitoyl GE: 1- palmitoylplasmenylethanolamine; 1-palmitoylplasmenyl E: 1-palmitoylplasmenylethanolamine.

A.

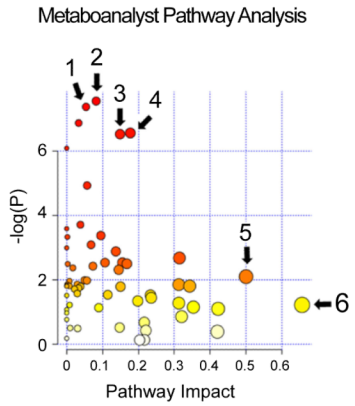

B.

Significant Pathway based on P-values/FDR

Pathway	Total Cmpd	Hits	Raw p	-log(p)	Holm adjust	FDR	Impact
1: Primary bile acid biosynthesis	47	5	0.00052212	7.5576	0.032371	0.018084	0.08221
2: Taurine and hypotaurine metabolism	20	4	0.00062594	7.3772	0.038146	0.018084	0.05395
3: Tryptophan metabolism	79	5	0.001406	6.567	0.082953	0.018084	0.1773
4: Histidine metabolism	44	4	0.0014584	6.5304	0.084587	0.018084	0.14863

Significant Pathway based on Impact factor

Pathway	Total Cmpd	Hits	Raw p	-log(p)	Holm adjust	FDR	Impact
5: Linoleic acid metabolism	15	1	0.29387	1.2246	1	0.39611	0.65625
6: D-Arginine and D-ornithine metabolism	8	2	0.12211	2.1028	1	0.29538	0.5

Figure 4. Metabolites altered in EAE compared to healthy group map to multiple biosynthetic pathways

A. Each of 80 KEGG pathways plotted according to Global Test p-value (vertical axis, intensity of color) and impact factor (horizontal axis, size of circle). **B.** Statistics for pathways with major change based on the p value (pathways 1-4) or on high impact (pathways 5-6).

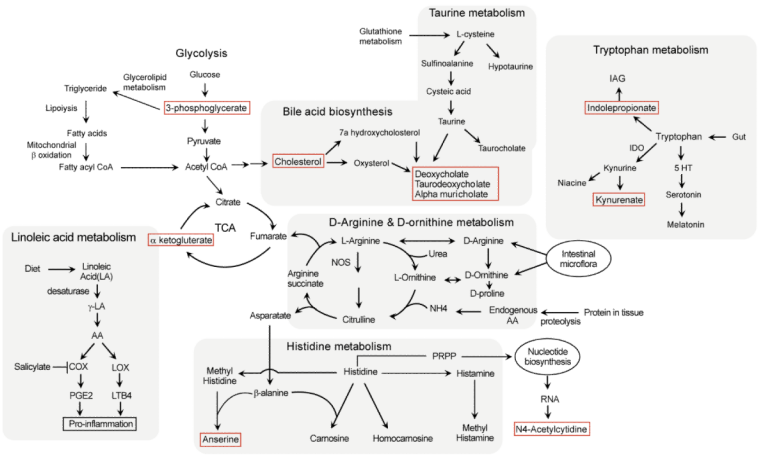

Figure 5. Perturbation of metabolic pathways in EAE compared to healthy group

Altered pathways summarized from KEGG and SMPDB reference pathways. Red nodes represent significantly altered metabolites (n=8 EAE and n=6 healthy; $p<0.05$, FDR<0.23).

Table 1

Up-regulated metabolites in plasma of EAE compared to healthy group .

Number	BIOCHEMICAL	SUPER_ PATHWAY	SUB_PATHWAY	PLATFORM	KEGG	T-stat	p value	q value
1	1-palmitoylglycerophosphoethanolamine	Lipid	Lysolipid	LC/MS Neg		6.072	5.57E-05	0.011
2	1-oleoylglycerophosphoethanolamine	Lipid	Lysolipid	LC/MS Neg		5.031	0.0003	0.027
3	1-eicosadienoylglycerophosphocholine*	Lipid	Lysolipid	LC/MS Pos		4.202	0.0014	0.027
4	1-linoleoylglycerophosphoethanolamine*	Lipid	Lysolipid	LC/MS Neg		2.999	0.0131	0.132
5	1-arachidoylglycerophosphocholine	Lipid	Lysolipid	LC/MS Pos		2.923	0.0151	0.132
6	1-palmitoylplasmenylethanolamine*	Lipid	Lysolipid	LC/MS Neg		2.254	0.0437	0.209
7	heptanoate (7:0)	Lipid	Medium chain fatty acid	LC/MS Neg	C17714	4.600	0.0007	0.027
8	pelargonate (9:0)	Lipid	Medium chain fatty acid	LC/MS Neg	C01601	3.167	0.0099	0.112
9	pentadecanoate (15:0)	Lipid	Long chain fatty acid	LC/MS Neg	C16537	3.014	0.0121	0.129
10	nonadecanoate (19:0)	Lipid	Long chain fatty acid	LC/MS Neg	C16535	2.482	0.0289	0.180
11	cis-vaccenate (18:1n7)	Lipid	Long chain fatty acid	GC/MS	C08367	2.401	0.0365	0.207
12	10-heptadecenoate (17:1n7)	Lipid	Long chain fatty acid	LC/MS Neg		2.312	0.0426	0.209
13	butyrylcarnitine	Lipid	Fatty acid metabolism (also BCAA metabolism)	LC/MS Pos		4.144	0.0022	0.032
14	cholesterol	Lipid	Sterol/Steroid	GC/MS	C00187	2.849	0.0149	0.132
15	beta-sitosterol	Lipid	Sterol/Steroid	GC/MS	C01753	2.599	0.0306	0.184
16	myo-inositol	Lipid	Inositol metabolism	GC/MS	C00137	2.299	0.0416	0.209
17	homostachydrine*	Xenobiotics	Food component/Plant	LC/MS Pos	C08283	4.949	0.0006	0.027
18	stachydrine	Xenobiotics	Food component/Plant	LC/MS Pos	C10172	4.340	0.0010	0.027
19	hippurate	Xenobiotics	Benzoate metabolism	LC/MS Neg	C01586	3.847	0.0029	0.039
20	equol sulfate	Xenobiotics	Food component/Plant	LC/MS Neg		2.832	0.0253	0.163
21	salicylate	Xenobiotics	Drug	LC/MS Neg	C00805	2.791	0.0183	0.139
22	benzoate	Xenobiotics	Benzoate metabolism	GC/MS	C00180	2.705	0.0238	0.158
23	indoleacrylate	Xenobiotics	Food component/Plant	LC/MS Neg		2.647	0.0227	0.156
24	isobutyrylcarnitine	Amino acid	Valine, leucine and isoleucine metabolism	LC/MS Pos		4.288	0.0012	0.027
25	isovalerylcarnitine	Amino acid	Valine, leucine and isoleucine metabolism	LC/MS Pos		3.148	0.0089	0.107
26	indolepropionate	Amino acid	Tryptophan metabolism	LC/MS Neg		2.756	0.0179	0.139
27	3-methyl-2-oxovalerate	Amino acid	Valine, leucine and isoleucine metabolism	LC/MS Neg	C00671	2.291	0.0430	0.209
28	3-(4-hydroxyphenyl)propionate	Amino acid	Phenylalanine & tyrosine metabolism	GC/MS	C01744	2.283	0.0420	0.209
29	alpha-tocopherol	Cofactors and vitamins	Tocopherol metabolism	GC/MS	C02477	2.714	0.0200	0.142
30	trigonelline (N'-methylnicotinate)	Cofactors and vitamins	Nicotinate and nicotinamide metabolism	LC/MS Pos		2.420	0.0340	0.198

Number	BIOCHEMICAL	SUPER_ PATHWAY	SUB_PATHWAY	PLATFORM	KEGG	T-stat	p value	q value
31	N4-acetylcytidine	Nucleotide	Pyrimidine metabolism, cytidine containing	LC/MS Pos		2.475	0.0446	0.209
32	methyl-beta-glucopyranoside	Carbohydrate	Fructose, mannose, galactose, starch, and sucrose metabolism	LC/MS Neg		2.207	0.0486	0.218

Table 2

Down-regulated metabolites in plasma of EAE compared to healthy group.

Number	Biochemical	Super_Pathway	Sub_Pathway	Platform	KEGG	T-stat	pvalue	qvalue
1	alpha-muricholate	Lipid	Bile acid metabolism	LC/MS Neg	C17647	−3.020	0.0181	0.1388
2	tetradecanedioate	Lipid	Fatty acid, dicarboxylate	LC/MS Neg		−4.012	0.0018	0.0290
3	deoxycholate	Lipid	Bile acid metabolism	LC/MS Neg	C04483	−4.695	0.0010	0.0268
4	taurodeoxycholate	Lipid	Bile acid metabolism	LC/MS Neg	C05463	−5.059	0.0008	0.0268
5	glycolate (hydroxyacetate)	Xenobiotics	Chemical	GC/MS	C00160	−3.553	0.0080	0.1026
6	citrulline	Amino acid	Urea cycle; arginine-, proline-, metabolism	LC/MS Pos	C00327	−4.007	0.0017	0.0290
7	kynurenate	Amino acid	Tryptophan metabolism	LC/MS Neg	C01717	−2.400	0.0410	0.2095
8	3-(4-hydroxyphenyl)lactate	Amino acid	Phenylalanine & tyrosine metabolism	LC/MS Neg	C03672	−2.717	0.0188	0.1388
9	1,5-anhydroglucitol (1,5-AG)	Carbohydrate	Glycolysis, gluconeogenesis, pyruvate metabolism	GC/MS	C07326	−5.327	0.0013	0.0268
10	3-phosphoglycerate	Carbohydrate	Glycolysis, gluconeogenesis, pyruvate metabolism	GC/MS	C00597	−2.869	0.0141	0.1322
11	alpha-ketoglutarate	Energy	Krebs cycle	GC/MS	C00026	−2.289	0.0460	0.2109
12	anserine	Peptide	Dipeptide derivative	LC/MS Neg	C01262	−2.208	0.0511	0.2235